Millimeter-Wave Radar Sensor for Automotive Intelligent Cruise Control (ICC)

Mark E. Russell, *Member, IEEE,* Arthur Crain, Anthony Curran, Richard A. Campbell, *Life Senior Member, IEEE,* Clifford A. Drubin, *Member, IEEE,* and William F. Miccioli

***Abstract*— If automotive intelligent cruise-control (ICC) systems are to be successful in the marketplace, they must provide robust performance in a complex roadway environment. Inconveniences caused by reduced performance during inclement weather, interrupted performance due to dropped tracks, and annoying nuisance alarms will not be tolerated by the consumer, and would likely result in the rejection of this technology in the marketplace. An all-weather automotive millimeter-wave (MMW) radar sensor is described that uses a frequency-modulation coplanar-wave (FMCW) radar design capable of acquiring and tracking all obstacles in its field of view. Design tradeoffs are discussed and radar-sensor test results are presented along with the applicability of the radar to collision-warning systems.**

I. Introduction

INTELLIGENT cruise control (ICC) uses forward-looking sensors to collect information about traffic and obstacles in the roadway ahead. It uses this information to maintain a constant headway or follow interval to a vehicle ahead that is being followed.

Remote-sensing technology has been associated with automotive applications since the 1960's [1]–[7]. Presently, the evolution of radar technology has afforded us the opportunity to create advanced automotive products using remote-sensing technology at a price that consumers will be willing to pay. Advances in gallium–arsenide monolithic-microwave integrated-circuit (MMIC) technology enable operation at millimeter wavelengths, providing reductions in size, weight, and production costs. Similarly, the availability of more powerful low-cost microprocessor integrated circuits (IC's) allows the implementation of sophisticated real-time software algorithms, which historically have required large and expensive computer platforms on which to run. The combination of these technological advances permits the development and introduction of a small low-cost sensor, providing the basis for a new class of automotive radar products.

A millimeter-wave radar sensor exploiting recent advances in MMIC and IC technology has been developed for ICC applications. For this purpose, it must perform two important functions. The first is to correctly locate a lead vehicle being followed, constantly differentiating between the lead vehicle and competing vehicles and roadside objects. The second is to report the distance, relative speed, and acceleration of the lead vehicle to the platform vehicle speed control unit with constant updates at a specified rate. The ability to collect, process, and keep track of information on the distance, relative speed, acceleration, and angular position of all objects in its field-of-view enables this sensor to correctly interpret situations which would otherwise result in faulty analysis of ambiguous data. Table I summarizes its performance specifications. The frequency of operation is chosen to be consistent with the automotive sensor-frequency allocation in Europe (and now in the U.S.). The field-of-view geometry is selected for operation on U.S. interstate multilane highways to provide effective acquisition and tracking of objects to greater than 75-m relative range on a 500-m minimum radius curve.

TABLE I
PERFORMANCE SPECIFICATIONS

Characteristic	Value
Operating Frequency	76-77 GHz
Waveform	FM-CW
Range	3-100+ meters
Range Accuracy	< 0.5 meters (3 sigma)
Relative Speed	< ± 160 Km/hr
Relative Speed Accuracy	< 1.5 Km/hr (3 sigma)
Update Rate	20 Hz
Field of View (Azimuth)	8.8 degrees
Field of View (Elevation)	4 degrees
Max. Targets Under Track	40
Interface	RS-232, High-Speed Parallel

II. Sensor System Design

There are several sensor types that have or could be used in automotive applications. Included among them are acoustic, optical (visual, laser, and infrared), and radar. The environment in which the sensor must operate plays an important role in the decision to pick one technique over another. The sensor should be able to adequately perform in any commonly encountered weather condition, including rain, snow, and fog. Its performance must not be catastrophically affected by the physical effects of inclement weather, such as water, ice, or mud buildup on the sensor face. While infrared and laser systems can penetrate fog and rain to some degree, they severely degrade in sensitivity with any buildup of foreign material on the sensor face. The effects of weather on visual light sensors are even more severe. Acoustic sensors are not sensitive enough to effectively perform at the required

Manuscript received March 24, 1997; revised August 15, 1997.

M. E. Russell, A. Curran, C. A. Drubin, and W. F. Miccioli are with Raytheon, Tewksbury, MA 01876 USA (e-mail: Mark-E-Russell@Res.Raytheon.com).

A. Crain, retired, was with Raytheon, Tewksbury, MA 01876 USA. He is now at 9 Surrow Drive, Framingham, MA 01701.

R. A. Campbell, retired, was with Raytheon, Tewksbury, MA 01876 USA. He is now at 2040 Main St., Concord, MA 01742.

Publisher Item Identifier S 0018-9480(97)08325-7.

TABLE II
SENSOR TRADEOFFS

· **Waveform**
✓ FMCW
- Pulse Doppler - Complex & Expensive
· **Antenna**
✓ Separate Tx/Rx (Bi-Static) - Dynamic Range, Sensitivity
- Single Antenna
- Quasioptical
- Waveguide
✓ Microstrip - High Performance, Low Profile (Minimum Volume), Low Cost
· **Antenna Scanning**
✓ Switched Beams
- Mechanical - Reliability Issues
- Frequency - Complexity (Waveform Limitations)
- Phase - Development Cost & Lead Time, Production Cost
· **Transmitter**
✓ Gunn Oscillator (Present Approach)
✓ HBT, PHEMT MMIC Oscillator (Planned Approach)
· **Receiver**
- Homodyne - Poor Noise Performance
✓ Heterodyne (Present Approach)
✓ Chopped Homodyne (Planned) - Less Complexity Than Heterodyne; Requires MMW LNA
· **Signal Processing**
✓ Digital Processor
- Analog Filters - Hardware Complexity & Cost

ranges. Radar performs well in all weather conditions likely to be encountered and tolerates the physical effects of weather without catastrophic consequences.

The choice of the radar band in which to operate was made considering the beam dimensions desired and the area available for the antenna in a typical application. This led to a fairly universal choice for a forward-looking sensor, reinforced by the recent federal assignment of the 76–77-GHz band for automotive applications. Radar at these frequencies performs well in fog and rain at rates up to at least 10 mm/h. Other bands can be, and are being, used. For example, short-range broad-beam X-band radars are used for side and rear warning systems where the actual position of the obstacle is not so important. The only importance is that an obstacle is there.

After the choices of a radar solution and the frequency of operation are made, there are several radar architectures and circuit design approaches to consider. Table II lists some of the tradeoffs made in shaping our solution to the problem. These will be elaborated upon in the following sections.

In order to keep the hardware and architecture relatively simple, keep the peak power down, and at the same time achieve robust performance, an FMCW approach was pursued as opposed to a more sophisticated pulse-Doppler implementation. A radar of this type has a relatively low peak-power output and can meet the range and velocity resolution requirements if a sufficiently large frequency deviation is used. Since the power level is low, it is possible to obtain MMIC subassemblies at a reasonable cost. The basic principle of an FMCW radar is that the frequency being transmitted is changed with time in a prescribed manner, so that by comparing the (time-delayed) received signal's frequency with a sample of the nondelayed transmit frequency, a measure of transit time can be obtained. In this specific design, the time-varying frequency is in the form of a linear ramp so that the range determination amounts to measuring the beat frequency between the transmit- and return-signal frequencies. The frequency so measured is equal to the slope of the frequency ramp multiplied by the time delay of the returned signal. Due to the constant velocity of electromagnetic radiation, the time delay is directly proportional to the range. In addition to the range-dependent beat frequency, the observed frequency also contains the Doppler frequency due to the relative velocity between the target vehicle and the platform vehicle. In order to separate and identify the two contributions to the frequency shift, a triangular frequency waveform is employed. For the positively sloped ramp the observed frequency is the difference between the range and Doppler frequencies; for the negatively sloped ramp it is the sum of the two. The solution of two simple linear equations using the up and down ramp measurements unambiguously yields both velocity and range.

III. SENSOR HARDWARE DESIGN

Fig. 1 shows a block diagram of the patent-pending sensor design, and Fig. 2 shows the physical package, a rectangular-shaped enclosure of dimensions 10 in wide $\times$ 6.5 in high $\times$ 5.5 in deep. The radar generates an FMCW waveform using an indium–phosphide (InP) Gunn-diode voltage controlled oscillator (VCO) generating +8 dBm at the output of the multibeam switch to the antenna at the fundamental radiating frequency. Samples of the output supply the receiver with its first local oscillator and provide feedback for the frequency control circuits. A Gunn-diode oscillator was chosen as the source for this radar because it is available technology; it provides sufficient power at the transmit frequency, it is easily tuned over the required bandwidth, and it has good noise performance. MMIC oscillators using either heterojunction bipolar transmitter (HBT) or pseudomorphic high electron-mobility transistor (PHEMT) technology are under development and are planned for use in the next-generation design. The waveform consists of positive and negative slope frequency ramps and a fixed-frequency intervals. During the fixed-frequency interval, the VCO is phased locked to a harmonic of a clock oscillator. The ramp portions are linearized using a sample of the VCO output frequency fed to an SAW delay-line interferometer producing an output signal proportional to the slope of the ramp. This signal's frequency is compared to a fixed reference

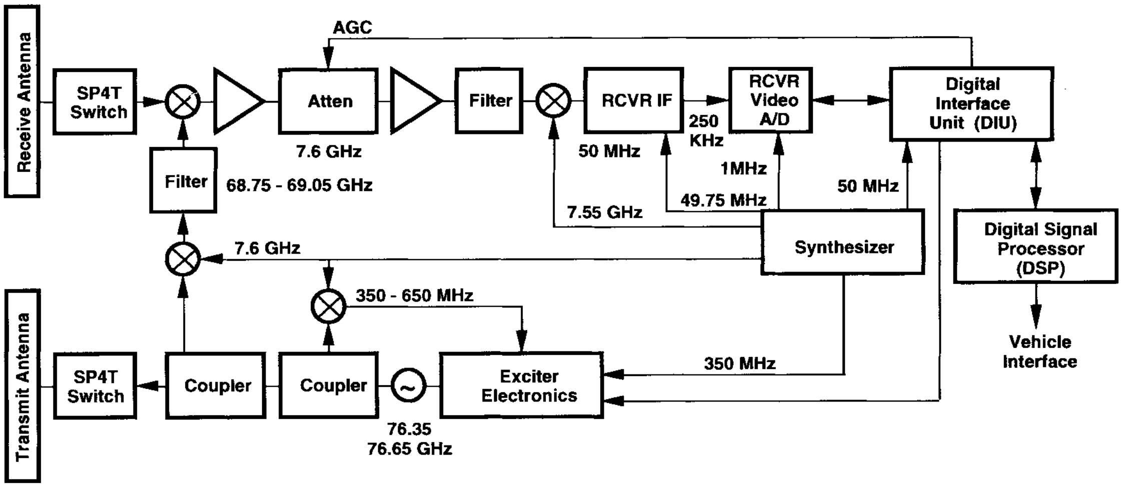

Fig. 1. Radar-sensor block design.

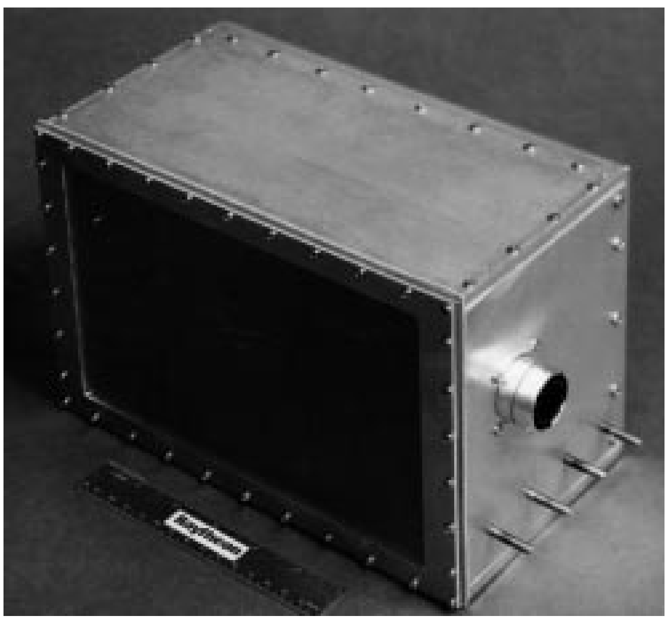

Fig. 2. Radar-sensor package.

to generate an error signal that corrects the VCO slope. A block diagram of this circuit is shown in Fig. 3. The requirement for linearity in the frequency ramp is 0.05%, based on the desire for a stable and accurately measured beat frequency from the target. Uncontrolled departures from linearity would smear the received signal in frequency. The signal processed filter is approximately 1.4 kHz (equivalent to approximately 0.5 m) and the filter separation is approximately 1 kHz. The linearity constraint keeps the return frequency variation to less than 100 Hz.

Relevant characteristics of the waveform are shown in Fig. 4. The up, down, and CW intervals are each 1.024 ms long and are sampled at a 1-MHz rate to yield 1024 real samples. With $\cos^2$ (Hanning) weighting, this provides a range resolution of 0.78 m and a range-rate resolution of 2.8 m/s. Assuming a minimum signal/noise ratio of 11 dB and the processing of two ramp pairs (required to initiate a track file), range and range rate measurement accuracies (1σ) are 0.11 m and 0.39 m/s, respectively. Typically, signal/noise ratios for vehicular targets are in excess of 20 dB within the 100-m operating range of the radar sensor. This results in 1σ accuracies of 0.04 m in range and 0.14 m/s in range rate.

The radar uses a patented bi-static antenna system obtaining approximately 80 dB of transmit-receive isolation to prevent receiver desensitization. The two antennas are printed circuits mounted on the front face of the radar enclosure and covered by a flat radome. The antenna produces several overlapping beams to cover the field of view and employs sequential lobing techniques in order to locate targets in azimuth. The novel printed-circuit antenna consists of a Rotman–Turner lens beamformer and an array of series-fed patch antennas built on a 5-mil-thick soft-substrate material. The lens forms a beam by distributing the energy incident at a feed point (in a proper manner) to the elements of the antenna array. Beam position is controlled by electronically switching the Rotman–Turner lens feed point. This changes the phase and amplitude distribution of energy to the patch array, steering the beam in azimuth. The approach provides both fine spacial resolution and a broad field of view, while minimizing volume and aperture size. Directive beams are employed for both transmit and receive in order to maximize directive gain and to provide two-way suppression of object returns occurring in the antenna sidelobes. With this approach we have built antennas that provide an azimuth coverage of 8.8° using four beams and 15.4° using seven beams, each with an individual beam width of 2°.

The radar is currently instrumented with a four-beam antenna The elevation beamwidth is fixed at 4° to allow for reliable detection of roadway objects regardless of vehicle pitch and variations in road inclines. A seven-beam antenna (shown mounted on an evaluation fixture) and its performance is shown in Fig. 5. The ICC acquisition/track antennas are shown on the vertical face of the fixture. The thin flexible substrate is wrapped around a U-shaped support. The radar-sensor package uses the internal volume to house the radar's electronic components. The Rotman–Turner lens and feed structure for the top antenna are clearly visible. Underneath the structure is an identical feed for the lower antenna. Also pictured in the photograph of the antenna are three additional

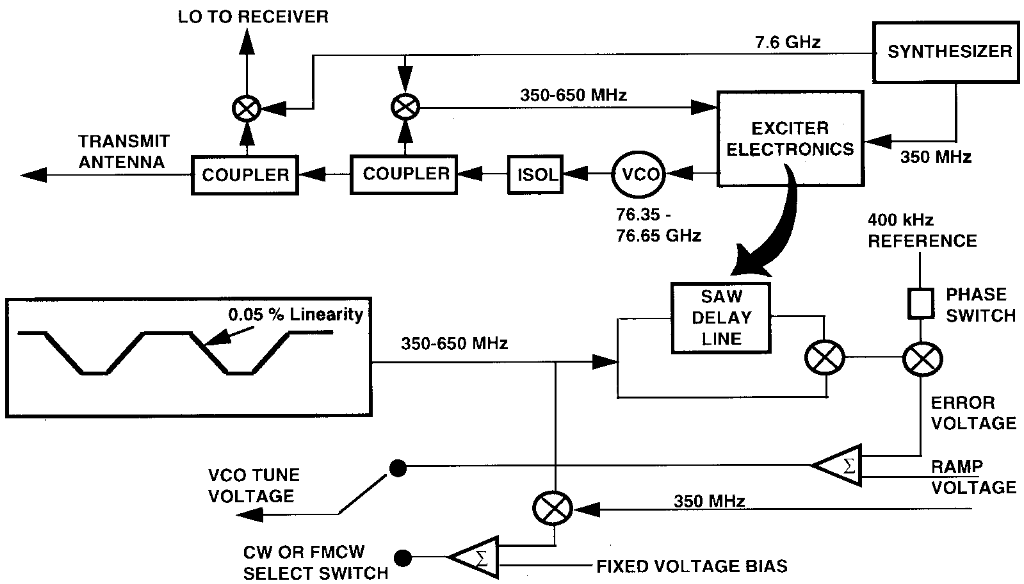

Fig. 3. Waveform generation.

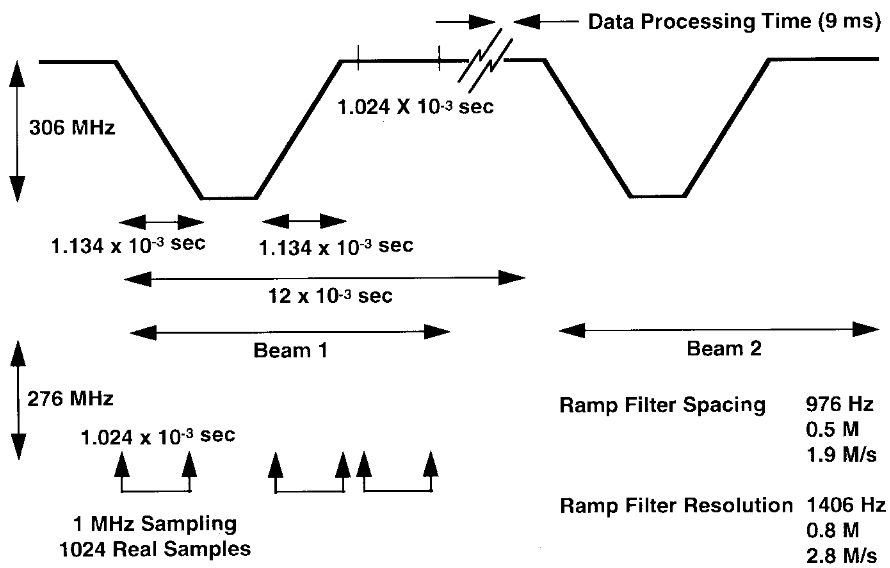

Fig. 4. Waveform characterization.

elements not connected to a Rotman–Turner lens. These are used for automatic alignment of the sensor on the vehicle.

The measured patterns exhibit a smooth rolloff in gain from the center to the outer beams due to differences in feed-path lengths on the planar substrate; transmission-line losses at this frequency are approximately 0.8 dB/in. Small differences in gain between beams is easily compensated for by the signal-processing software so that errors in interpolating the angle of an object detected in adjacent beams are minimized. The decrease in gain in the several beams relative to adjacent neighbors is due to a slight phase misalignment correctable with an adjustment in the shape of the lens. The design goal for sidelobe performance was greater than 20 dB. In several of the beams this was not achieved. This is attributed to small errors in the Rotman–Turner design code and is expected to be corrected with minor artwork changes in subsequent designs.

The antenna's ideal area gain is 37.5 dB isotropic (dBi). Losses associated with illumination, mismatch, and transmission line ohmic contributions (including the Rotman–Turner lens) are approximately 10 dB. Although this might appear to be excessive, one must realize that it is sufficient for the application without putting unreasonable constraints on transmit power or receiver front-end noise figure.

Performance is just one aspect of this antenna approach that makes it uniquely suited to the application. Because it is thin and flexible, it can be easily formed around the electronics, minimizing the physical volume required to perform its function. At the same time, it is repeatedly and reliably produced using low-cost automated processes. A mechanically scanned antenna design was considered in the early stages of development, but eliminated as a candidate due to concerns about reliability. A frequency-scanned antenna was

TABLE III
CHIRP WAVEFORM PROCESSING SPECTRUM

· Chirp Slope	270 kHz/microseconds
· Delay for 100M	2/3 microseconds
· Frequency Delta @ 100M	+180 kHz - Down Chirp
	-180 kHz - Up Chirp
· Maximum Platform Velocity (100 MPH)	+23 kHz Doppler
· Maximum Target/Clutter Range	-23 kHz to +226 kHz - Down
Chirp	
	+23 kHz to -226 kHz - Up
Chirp	
· Signal Spectral Width	249 kHz
· IF Carrier	250 kHz
· Sampling Rate	1 MHz

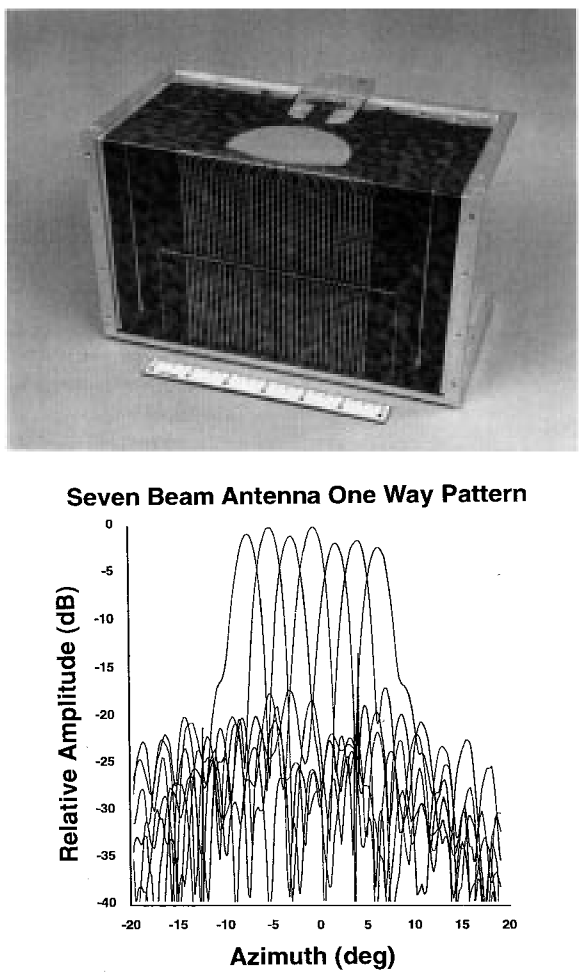

Fig. 5. Antenna design and performance.

eliminated due to the limitations it imposes on the waveform. Though probably the most appealing technical solution is a phase-scanned approach, the technology at millimeter-wave frequencies is in its infancy.

The receiver design is superheterodyne. No RF preamplification is required to achieve the necessary signal/noise ratio (of the order of 10 dB) for the detection of vehicular targets (including motorcycles) within the 100-m range. The radar return is converted down in frequency to a final IF of 250 kHz. As shown in Table III, range offset and Doppler are contained within a frequency band ± 250 kHz on either side of the IF frequency. The output of the receiver is fed to a 12-b analog-to-digital converter clocked at 1 MHz, satisfying Nyquist sampling criteria, which becomes the input to the digital processor. Although it introduces some hardware complexity, the superheterodyne approach was chosen for the present design in order to achieve the required noise figure. Though less complex and expensive, a simple homodyne receiver is out of the question for this application due to the severe degradation of noise figure below baseband frequencies of 1 MHz. A chopped homodyne approach is a viable alternative being developed for the next-generation design. Like the simple homodyne, the chopped homodyne receiver eliminates the microwave IF and associated local oscillators. However, it does this without sacrificing noise performance by shifting the detected output beyond the $1/f$ noise region of the downconversion mixer. However, in order to achieve receiver noise figures equivalent to that of a superheterodyne receiver, it is necessary to introduce a low-noise preamplifier ahead of the downconversion mixer to overcome the loss in signal power caused by the chopping process.

The current radar-sensor digital signal processor consists of two Texas Instruments TMS320C30 IC's, and associated logic, memory, and buffers (see Fig. 6) mounted on a 6 in $\times$ 9 in six-layer printed wiring board (PWB) separate from the sensor enclosure. One processor is dedicated to functions that support data recording and display (which is required only for engineering evaluation), while the other performs the essential radar-sensor operations. It takes less than 12 ms to collect, process, and display data measured at each beam position. Therefore, for a seven-beam system, data latency (time between radar updates) is less than 84 ms for an object currently being tracked. For a newly detected object, the latency is less than 168 ms because objects entering the radar field of view require two dwells at each beam position to assess validity and establish a track file. The next-generation design will reduce the hardware to a single processor on a surface-mount printed-wiring board within the radar-sensor package.

Analysis of received power levels from vehicles of various cross sections and from clutter (see Fig. 7) shows that the radar's sensitivity is sufficient to detect a vehicle as small as a motorcycle (1 m^2) at 100-m range, and that the dynamic range

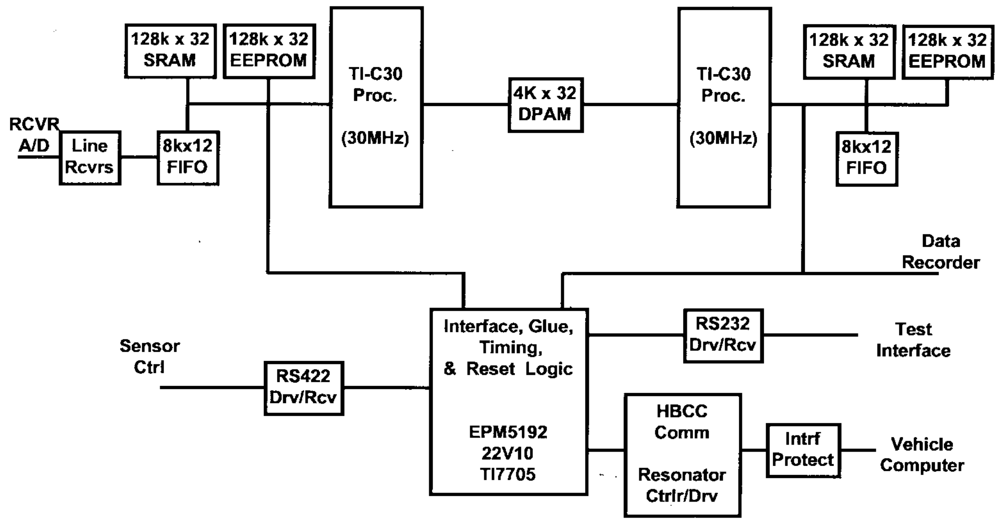

Fig. 6. Digital signal processor architecture.

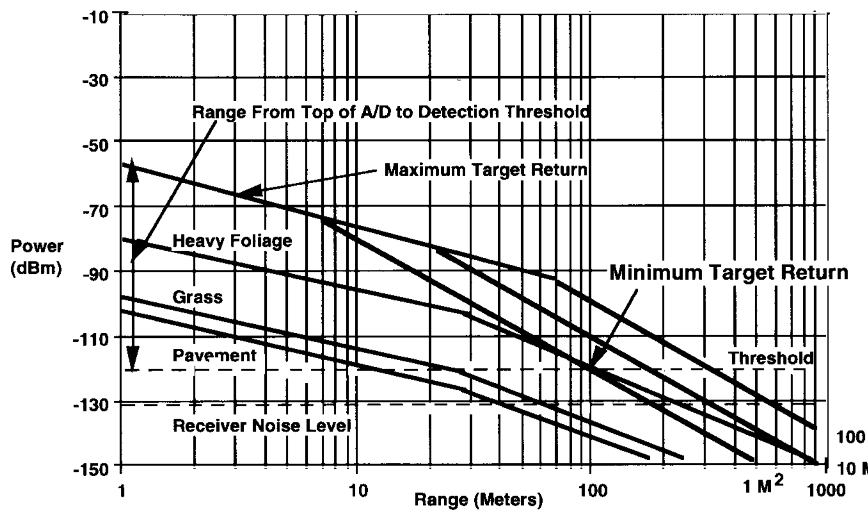

Fig. 7. Signal and interference levels.

of the receiver is sufficient to accommodate the entire range of expected signal returns.

IV. Algorithms

The patent-pending algorithms used in the digital processor track all the targets in the field of view (as many as ten objects in each beam). Based upon current data and the recent history of a given target, they predict each target's range, range rate, and acceleration at the time of the next radar action. Angular information is derived from the presence of the target in different (azimuth) antenna beams. The radar chooses the nearest target, satisfying certain acquisition criteria, as the lead vehicle. The radar then reports this vehicle's spatial parameters to the platform's computer.

It is essential to distinguish curves from lane changes. A lead vehicle in a curve should be followed, but one that leaves the platform vehicle lane should be dropped. Lane estimation uses platform yaw rate, moving vehicle tracks, and stationary object tracks. These data are used in three independent lane estimators, each of which determines an

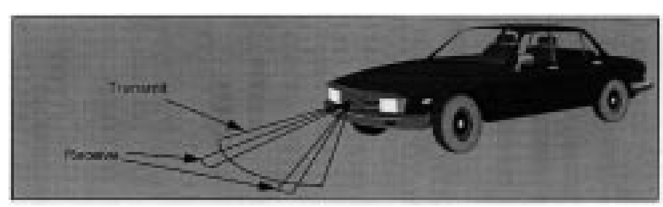

Fig. 8. Sensor self alignment.

estimate of the lane ahead of the platform vehicle and an associated uncertainty. These estimates are then statistically fused to create a composite lane estimate.

V. Alignment

Because it is important to maintain alignment of the antenna boresight to the platform vehicle longitudinal axis the sensor incorporates an electronic self-alignment feature. This is accomplished with three additional antenna elements. The transmit antenna consists of radiating elements of the same design as one of the ICC acquisition/track antenna elements.

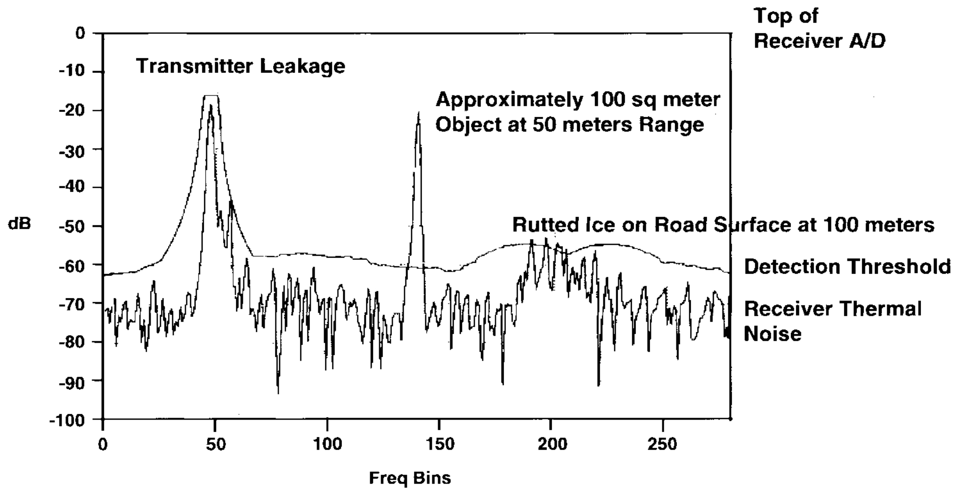

Fig. 9. Spectral response of radar signal returns.

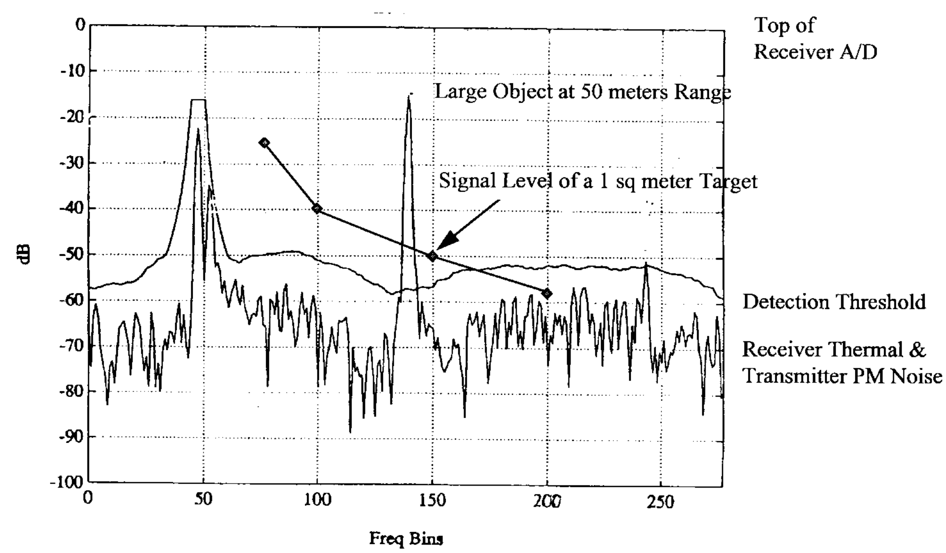

Fig. 10. Effect of transmitter P.M. noise on receiver sensitivity.

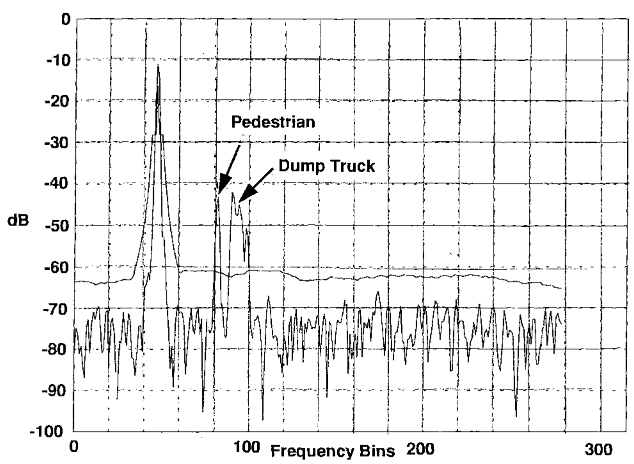

Fig. 11. Data illustrating the radar sensor's ability to resolve targets in range.

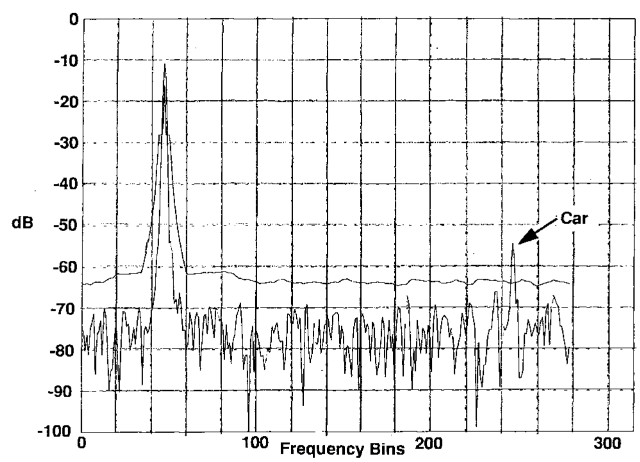

Fig. 12. Data illustrating the radar's sensitivity at maximum range.

It radiates a horizontal beam onto the ground in front of the vehicle at 45° from the horizontal. The receive antenna is a traveling-wave design which produces a vertical fan beam with approximately a 2° beamwidth aimed to the right or left of the vehicle center line at an angle of approximately 45°. The right or left position of the receive-antenna beam depends

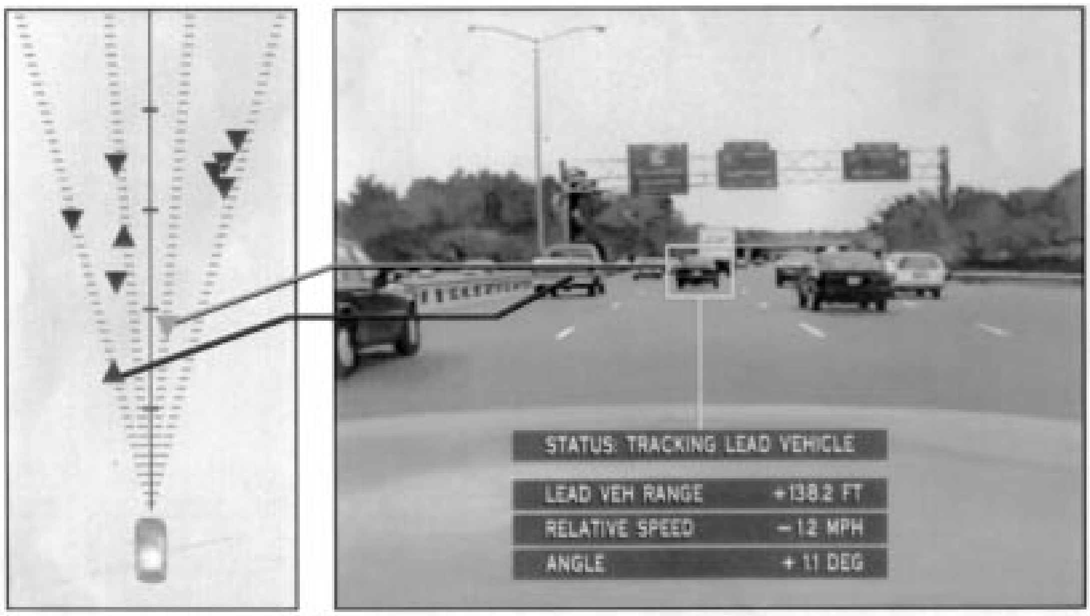

Fig. 13. Real-time tracking display.

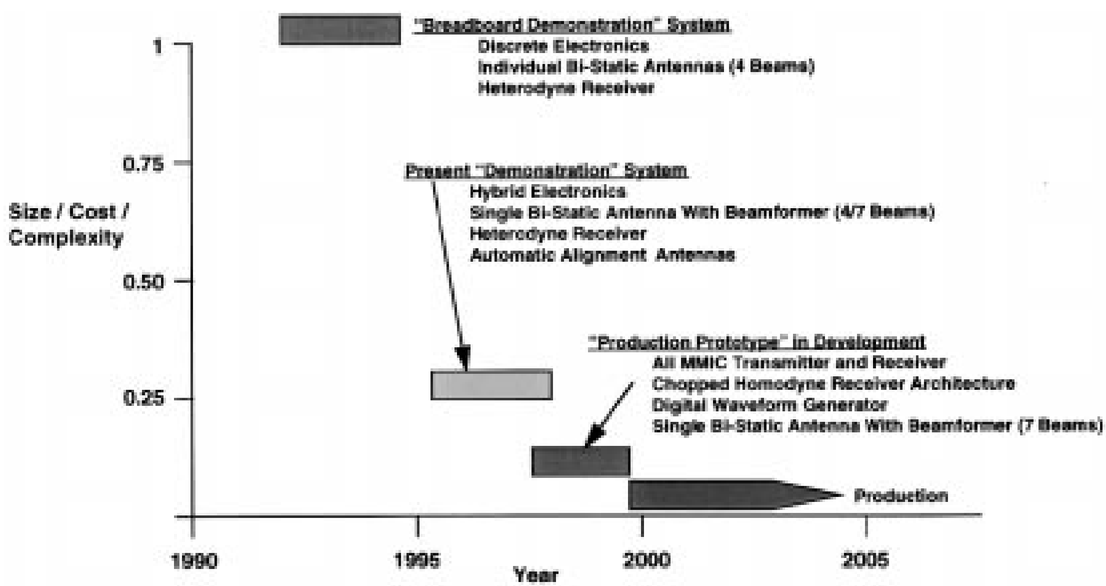

Fig. 14. Evolution of ICC radar-sensor development at Raytheon.

upon which end the receive antenna is driven. The driven end is switch selectable. The transmit and receive beams intersect at one of two spots (determined by the switch state) on the road in front of the vehicle. Doppler offsets from the two received signals yield the information required to calculate the sensor's normal compared to the vehicle's line of travel for correction in the signal processor. The concept is illustrated in Fig. 8. Fig. 5 shows the alignment beam antennas located on either side of and between the two acquisition/track antenna arrays.

VI. Testing

Initial testing included detection and tracking of stationary corner reflectors and moving vehicles from a stationary platform in order to verify range, range-rate, and angle accuracies. Fig. 9 shows a typical signal return (after fast Fourier transform (FFT) processing) of a corner reflector 50 m from the radar. Shown also in this example is feedthrough of the transmit signal to the receiver at zero range and small returns at 100 m from rutted ice and snow on the road surface. The requirement for adequate transmit-to-receive isolation is graphically illustrated here. If a single antenna and duplexer circulator were used, the feedthrough level would cause the receiver to saturate. With 80 dB of isolation, this (bi-static) system has greater than 15-dB margin.

Fig. 10 illustrates the effect of transmitter P.M. noise on the received signal spectrum. In this example, transmitter-noise sidebands reflecting off of a large corner reflector at approximately 50-m range raise the receiver noise floor by as much as 10 dB ahead of and behind the location of the large object. Though at first glance this may seem disturbing, it has no serious effect on performance because smaller targets of interest that are closer in range will have returns that exceed the elevated noise threshold.

Fig. 11 illustrates the ability of the radar to resolve targets in range. A pedestrian standing a car length behind a dump truck and between the dump truck and the forward-looking radar sensor is clearly and distinctly resolved despite their difference in size. Also resolvable in range are the various scattering locations on the truck itself, which has a number of protrusions along its longitudinal extent.

Fig. 12 is an example showing the sensitivity of the sensor to objects at its maximum designed range. The signal return of a small automobile (approximately 10-m^2 cross section) is clearly detected 10 dB above the detection threshold as predicted by the analytical predictions in Fig. 7.

Extensive open-loop testing on a moving platform was performed on U.S. interstate-type highways and included all vehicle types, weather conditions, and clutter environments. Excellent vehicle tracking performance was observed for cars, trucks, motorcycles, and pedestrians. The instrumentation included a computer, a video camera and recorder, a data recorder, and a display. Fig. 13 shows a freeze frame from the real-time tracking display used for open-loop sensor testing. With this system, sensor range, relative speed, and angle to the lead-vehicle are reported numerically, positioned below the video image of the roadway ahead. A cursor, overlaid with the video image, provides a constantly updated visual indication of the vehicle under track. Also included on the display screen is a real-time graphical representation of the sensor's field of view using triangles to represent the position of all obstacles under track. Horizontal tick marks represent distances of 25, 50, 75 and 100 m, respectively. The direction of each obstacle's radial velocity is indicated in the diagram by the direction the triangle is pointing (opening or closing range).

VII. Design Evolution

The design basis for the previously described system hardware and algorithms draws upon Raytheon's long history and experience designing radar systems and radar-guided missile seekers for severe military operational scenarios and environments. Raytheon's approach has been to first design a system that performs without compromise, and then to evolve and improve upon it to enhance producibility and reduce cost without sacrificing performance. Fig. 14 illustrates that development path and timetable to a commercially available product. Raytheon is currently working on a new version of the sensor design to reach production cost goals. This will be accomplished by introducing MMIC technology in the transmitter and receiver front end, employing a simpler (chopped homodyne) receiver downconversion, and by using digital synthesis techniques for signal generation.

VIII. Conclusion

Raytheon has developed a forward-looking automotive radar sensor for ICC. The requirements for these applications are driven by the need for high resolution spatial selectivity in range, relative speed, and angle. The recognition of spatial selectivity as a key element in a robust ICC system has yielded a design whose performance will also meet the needs of forward-looking collision-warning systems.

Raytheon is currently working on a new version of the sensor design to reach production cost goals. The approach is to introduce MMIC technology in the transmitter and receiver front end, and to employ a simpler (chopped homodyne) receiver downconversion.

Acknowledgment

The authors would like to thank R. Walker, S. Huettner, and J. Birch for their significant design contributions, R. Mello for his help in assembly and integration, and T. Coletti for his test support.

References

[1] O. K. Nilssen, "New methods of range measuring Doppler radar," *IRE Trans. Aerosp. Navig. Electron.*, vol. ANE-9, pp. 255–265, Dec. 1962.

[2] D. M. Grimes and T. O. Jones, "Automotive radar: A brief review," *Proc. IEEE*, vol. 62, pp. 804–822, June 1974.

[3] T. O. Jones and D. M. Grimes, "Automotive station keeping and braking radars: A review," *Microwave J.*, vol. 18, no. 10, pp. 49–53, Oct. 1975.

[4] P. Lowbridge, "Low cost millimeter wave radar systems for intelligent vehicle cruise control applications," *Microwave J.*, vol. 38, no. 10, pp. 20–33, Oct. 1995.

[5] J. Woll, "VORAD collision warning radar," in *IEEE Int. Radar Conf.*, Alexandria, VA, May 1995, pp. 369–376.

[6] K. W. Chang *et al.*, "Forward-looking automotive radar using a W-band chip transceiver," *IEEE Trans. Microwave Theory Tech.*, vol. 43, pp. 1659–1668, July 1995.

[7] L. Eriksson and B. As, "High performance automotive radar for automotive AICC," *IEEE Int. Radar Conf.*, Alexandria, VA, May 1995, pp. 380–385.

Mark E. Russell (S'80–M'83) received the B.S.E.E. and the M.S.E.E. degrees from the University of Massachusetts, Amherst, in 1983 and 1984, respectively.

He is currently the Manager of Microwave Systems, Electronic Systems Laboratories, Raytheon, Tewksbury, MA, where he is responsible for advancing the state of the art in microwave technology, including antennas, solid-state transmitters, receivers, low-noise sources, photonics, millimeter-wave systems, quasi-optics, and radomes for both military (missile seekers, ground and airborne radars, satellite and terrestrial communications) and commercial (marine and air-traffic-control radars, and satellite communications) programs.

Mr. Russell was the recipient of a Raytheon Scholarship, and was awarded the Raytheon Outstanding Inventor Award in 1993.

Arthur Crain received the B.S. degree in physics from Providence College, Providence, RI, in 1957.

From 1958 to 1966, he worked as a Physicist in the Microwave Laboratory, Frankfurt Arsenal, prior to joining the Missile Systems Division, Raytheon, Tewksbury, MA. For the last 29 years, he has participated in the design and development of coherent airborne and ground-based radar systems, primarily for defense applications. In 1995, he retired from full-time employment, but has continued to provide system engineering-consultant services in support of ICC sensor development. He holds six U.S. patents.

Anthony Curran received the B.S.E.E. and M.S.E.E. degrees from Rensselaer Polytechnic Institute, Troy, NY, in 1989 and 1992, respectively.

He is currently working in the System Design Laboratories' System Concepts, Design and Simulation Department, Raytheon, Tewksbury, MA, where he is involved in algorithm design, analysis, and test for various missile guidance systems, automatic tracking systems, automotive radar system, and automated defensive systems.

Mr. Curran was the recipient of the Raytheon Miccioli Scholarship and was awarded the Raytheon Inventor's Award in 1994.

Richard A. Campbell (S'47–A'51–SM'56–LSM'92) received the B.A. degree from Washington University, St. Louis, MO, in 1952, and the M.S. degree from the University of Rochester, Rochester, NY, in 1954, both in physics.

From 1954 to his retirement in 1996, he worked at Raytheon, Tewksbury, MA, in the design and development of radar subsystems, with particular emphasis on radar transmitters, exciters, and test equipment. His primary interests were in the generation of low-noise microwave signals for local oscillators and radar exciters. He holds several patents.

Clifford A. Drubin (M'76) received the B.E. degree in engineering science, from the State University of New York at Stony Brook, in 1969, and the M.S.E.E. degree from Northwestern University, Evanston, IL, in 1976.

He is currently the Manager of microwave source development, Raytheon Electronic Systems Laboratories, Tewksbury, MA. He possesses over 20 years experience in the radar field, which includes the design of antennas, low-noise sources, receivers, solid-state transmitters, and millimeter-wave systems.

William F. Miccioli received the B.S.E.E. degree from Tufts University, Medford, MA, in 1980, and the M.S.E.E. degree from the University of Massachusetts, Amherst, in 1985.

He is currently at Raytheon, Tewksbury, MA, working with automotive radar development. His professional experience also includes working in Raytheon's missile antenna design section, and on numerous missile application tasks in the microwave area, including front-end receivers, transmitters, and sources.